

*Supplementary for*

# Urban Aerosol Particle Size Characterization in Eastern Mediterranean Conditions

Tareq Hussein <sup>1,2,\*</sup>, Lubna Dada <sup>2</sup>, Simo Hakala <sup>2</sup>, Tuukka Petäjä <sup>2</sup> and Markku Kulmala <sup>2</sup>

<sup>1</sup> Department of Physics, The University of Jordan, Amman 11942, Jordan

<sup>2</sup> Institute for Atmospheric and Earth System Research (INAR), University of Helsinki, PL 64, FI-00014 UHEL Helsinki, Finland; [lubna.dada@helsinki.fi](mailto:lubna.dada@helsinki.fi) (L.D.); [simo.hakala@helsinki.fi](mailto:simo.hakala@helsinki.fi) (S.H.); [tuukka.petaja@helsinki.fi](mailto:tuukka.petaja@helsinki.fi) (T.P.); [markku.kulmala@helsinki.fi](mailto:markku.kulmala@helsinki.fi) (M.K.)

\* Correspondence: [tareq.hussein@helsinki.fi](mailto:tareq.hussein@helsinki.fi)

Received: 13 October 2019; Accepted: 10 November 2019; Published: date

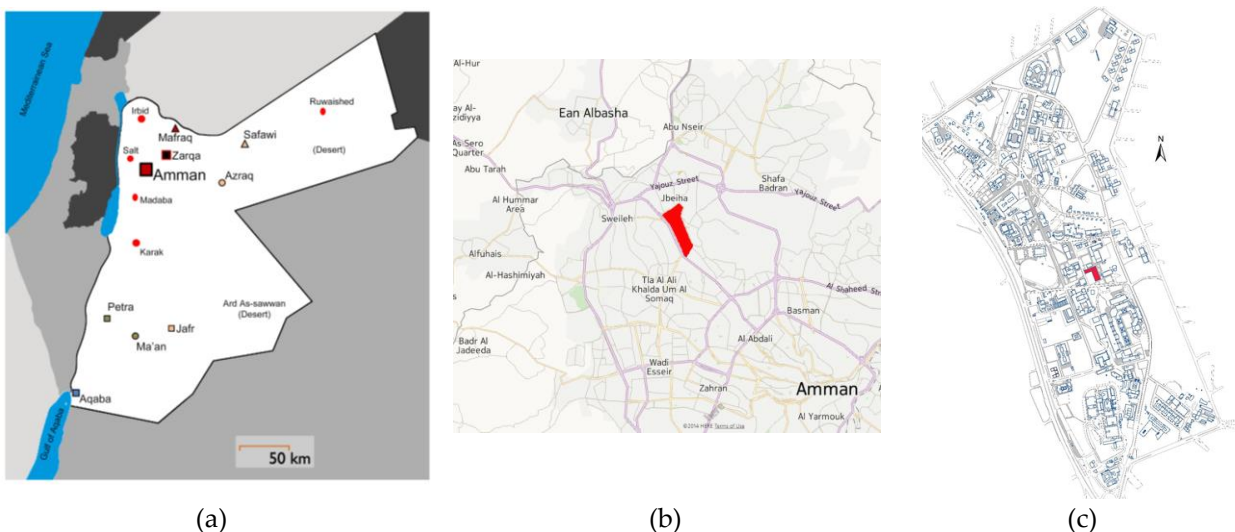


**Figure S1.** (a) A Map of Jordan showing the geographical location of Amman. (b) A Map of Amman showing the campus of the University of Jordan (shaded area) and (c) a detailed map of the campus of the University of Jordan, showing the sampling location (shaded area) in the middle of the campus.

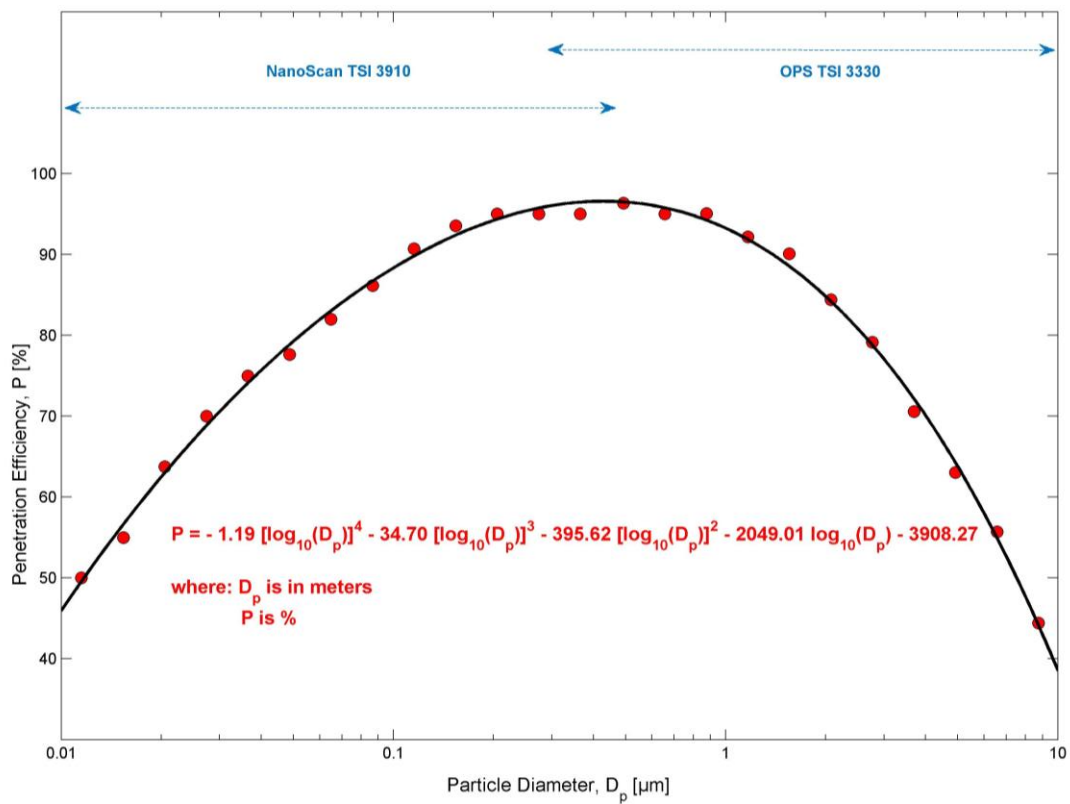


**Figure S2.** Experimental penetration efficiency through the sampling lines (tubing and diffusion drier).

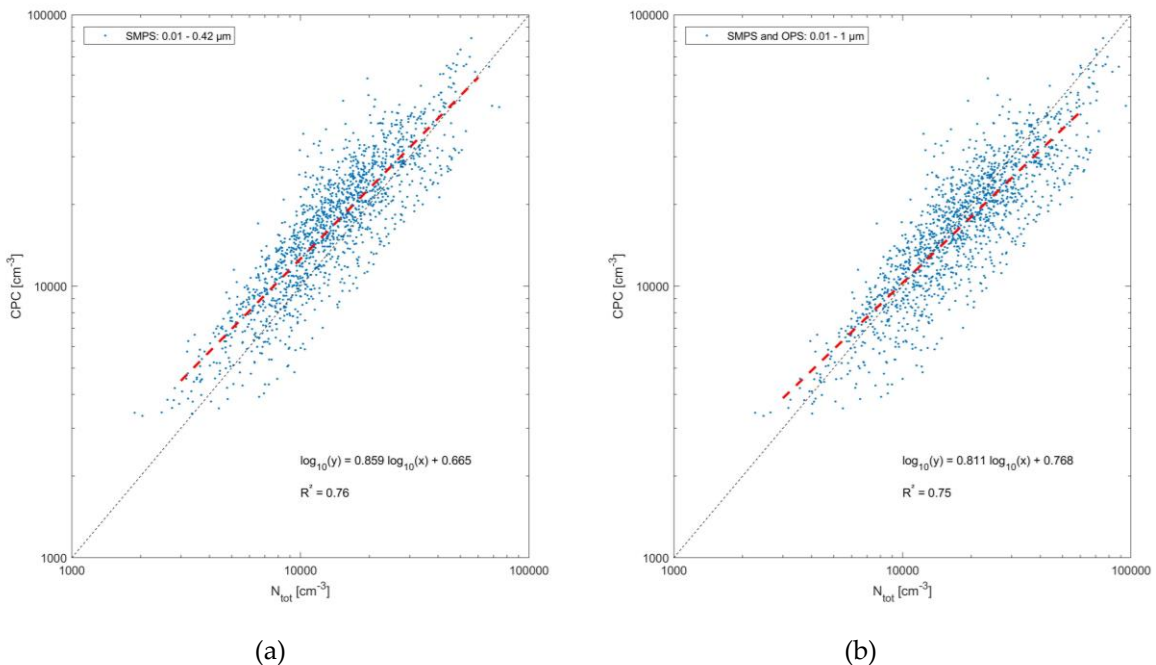


**Figure S3.** Regression between the number concentrations measured with the CPC versus (a) number concentration measured with the SMPS ( $D_p$  0.01–0.42  $\mu\text{m}$ ) and (b) number concentration derived from the combined particle number size distribution measurements (SMPS and OPS,  $D_p$  0.01–1  $\mu\text{m}$ ).

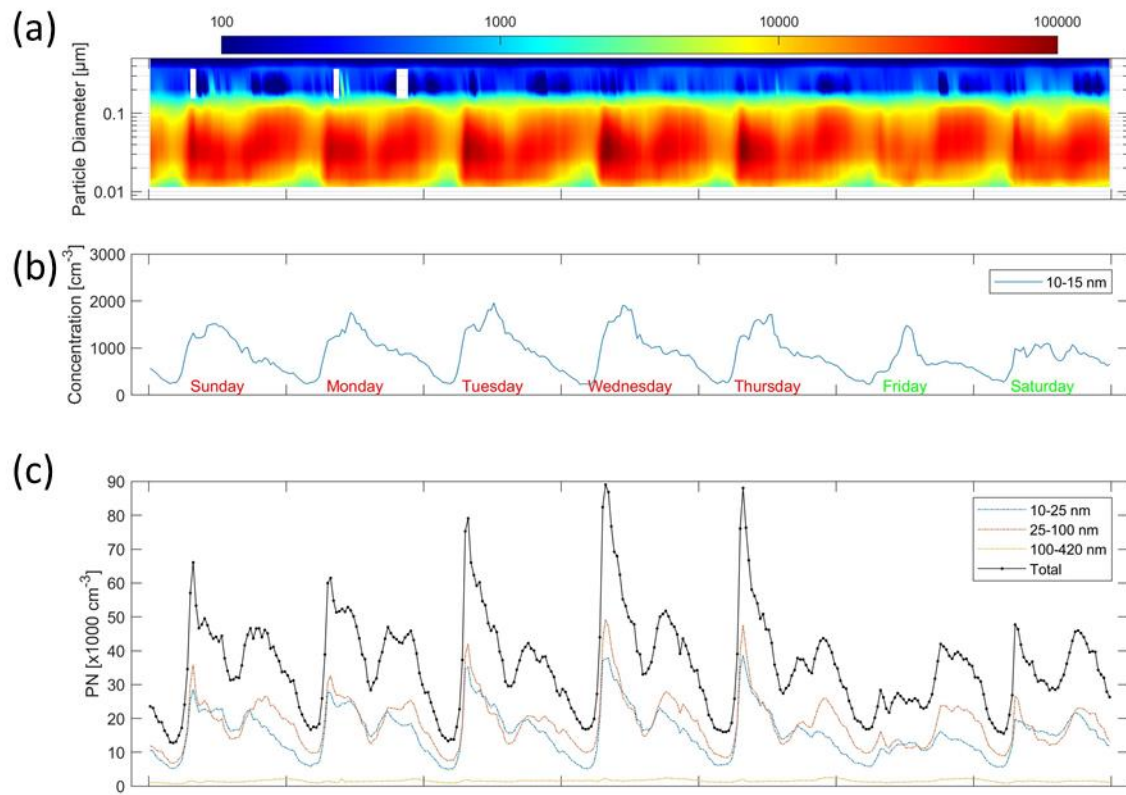


**Figure S4.** Weekly cycle and the diurnal pattern during a cold period (i.e. winter: December–February): (a) mean particle number size distribution spectra and (b–c) concentrations of different particle size fractions. The color bar represents  $dN/d\log(D_p)$  ( $\text{cm}^{-3}$ ).

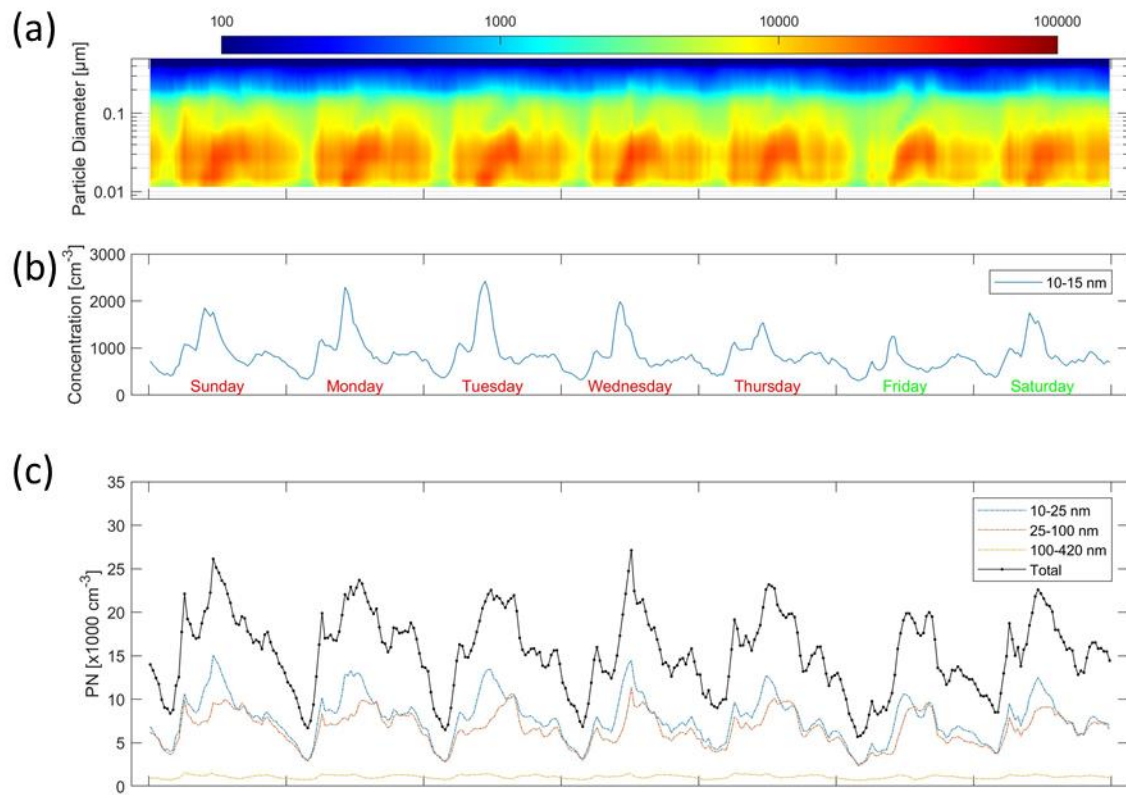


**Figure S5.** Weekly cycle and the diurnal pattern during a cold period (i.e. summer: May–August): **(a)** mean particle number size distribution spectra and **(b–c)** concentrations of different particle size fractions. The color bar represents  $dN/d\log(Dp)$  ( $\text{cm}^{-3}$ ).

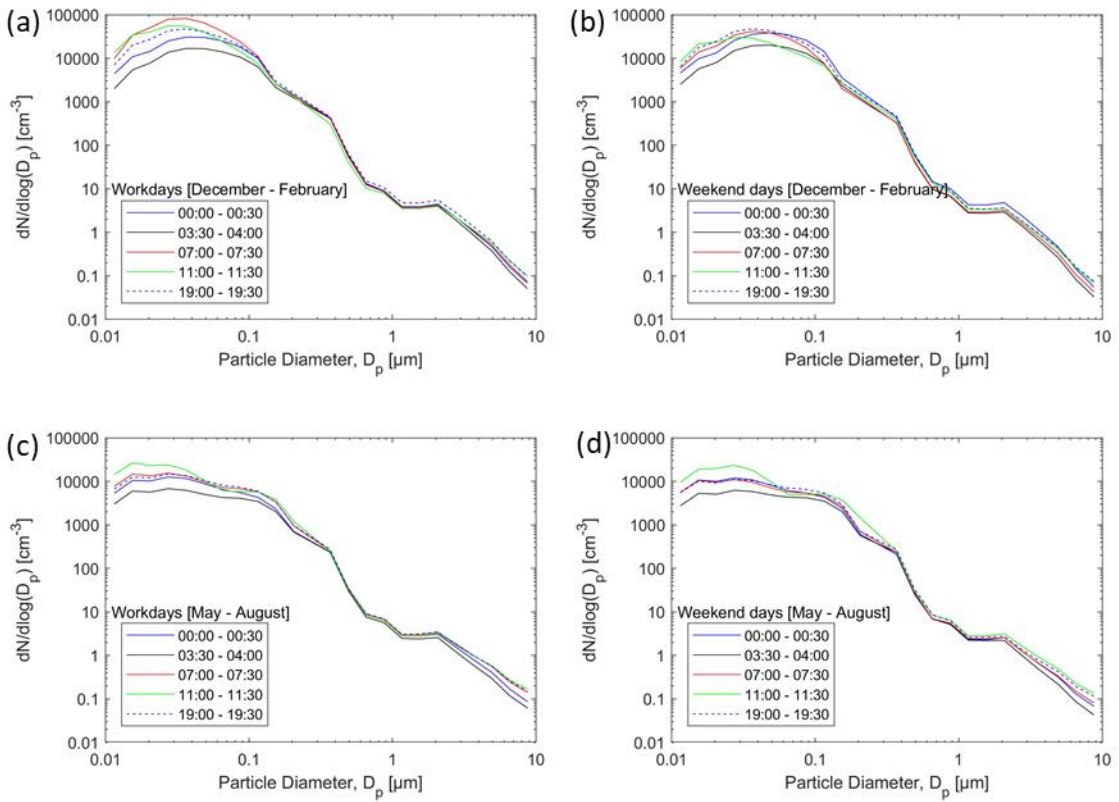


**Figure S6.** Mean particle number size distributions during (a,b) cold period (i.e. winter: December–February) and (c,d) warm period (i.e. summer: May–August). The mean distributions are shown for different times of the day on workdays (a,c) and weekend days (b,d).

**Table S1.** Monthly statistics for the main particle size fractions (concentrations in units of cm<sup>-3</sup>).

	Year	Month	Mean	STD	Min	5%	25%	Median	75%	95%	Max
Submicron 0.01–1 µm	2016	August	12,008	6079	2457	3821	7956	10,684	14,902	24,171	39,170
		September	14,310	8184	2269	4662	8595	12,312	18,549	29,909	57,844
		October	21,241	11,950	2708	6069	13,180	18,652	26,624	44,895	88,372
		November	27,686	18,177	3314	6288	14,280	22,941	37,266	65,174	101,684
		December	37,007	22,983	3238	7845	20,003	34,171	48,858	78,212	148,735
	2017	January	37,356	24,109	2920	8634	19,471	33,920	49,437	74,830	213,713
		February	32,501	18,352	4939	8479	18,712	29,607	43,091	68,023	123,148
		March	23,760	13,691	3356	6804	13,505	20,847	30,938	50,955	91,391
		April	19,745	11,869	4245	6814	12,270	17,394	24,540	41,421	141,512
		May	17,935	8709	2325	6385	11,443	16,655	22,578	33,825	57,065
		June	15,548	8921	3706	5665	9010	13,058	19,754	34,170	56,820
		July	16,247	9200	2170	4745	9805	14,245	21,042	33,886	60,186
Ultrafine 0.01–0.1 µm	2016	August	8050	4190	1316	2363	5260	7088	10,119	16,539	24,254
		September	9704	5651	1271	3033	5709	8452	12,398	20,726	39,384
		October	14,467	7994	1707	4178	9132	12,673	18,098	29,546	60,417
		November	18,923	12,183	2336	4357	9971	15,976	25,488	43,381	68,381
		December	25,795	15,805	2164	5434	14,239	23,882	33,953	55,163	99,753
	2017	January	25,886	16,657	1856	5930	13,485	23,622	34,713	51,814	149,861
		February	22,496	12,785	3384	5732	13,016	20,635	29,765	47,315	83,275
		March	16,461	9396	2142	4712	9571	14,527	21,088	35,312	61,735
		April	13,769	8123	2770	4704	8567	12,157	17,040	28,607	95,181
		May	12,441	5897	1550	4347	8035	11,693	15,700	23,819	38,512
		June	10,742	6007	2502	3907	6341	9164	13,462	23,359	35,194
		July	11,185	6266	1158	3239	6832	9861	14,281	23,419	41,020
Accumulation 0.1–1 µm	2016	August	1337	447	138	653	1044	1326	1594	2134	3056
		September	1216	451	111	606	900	1172	1470	2035	3458
		October	1360	842	102	468	834	1192	1636	2781	9005
		November	1385	1020	141	280	815	1183	1559	3613	6362
		December	1413	1120	87	262	658	1140	1849	3568	8521
	2017	January	1472	1087	80	345	804	1214	1856	3421	8432
		February	1632	1158	198	536	938	1329	1958	3647	9687
		March	1226	691	217	435	752	1104	1538	2355	5052
		April	1148	614	26	497	786	1034	1350	2176	5745
		May	1009	442	184	449	728	940	1212	1781	5137
		June	937	368	28	351	718	920	1118	1572	3112
		July	1076	409	23	456	793	1067	1322	1752	2793
Coarse 1–10 µm	2016	August	1.2	0.4	0.3	0.7	1.0	1.2	1.4	1.9	2.3
		September	1.3	1.2	0.2	0.5	0.7	1.0	1.3	3.8	9.9
		October	2.5	1.4	0.5	0.7	1.5	2.4	3.3	5.1	10.9
		November	3.8	4.1	0.3	0.7	1.5	2.9	4.5	10.8	32.4
		December	1.8	2.0	0.0	0.3	0.9	1.2	1.8	5.9	16.3
	2017	January	2.0	2.3	0.1	0.3	0.7	1.2	2.4	6.6	17.6
		February	2.2	2.5	0.1	0.2	0.7	1.4	2.9	6.4	19.6
		March	3.3	4.7	0.3	0.5	1.0	1.7	3.1	13.9	37.9
		April	3.3	5.1	0.3	0.6	1.1	1.6	3.2	12.0	45.8
		May	2.4	1.9	0.2	0.5	1.1	1.8	3.3	5.4	16.1
		June	0.9	0.6	0.1	0.3	0.6	0.8	1.0	1.8	4.9
		July	1.4	0.7	0.3	0.6	0.9	1.3	1.6	3.0	6.3